Analytical and Bioanalytical Chemistry (2020) 412:6121–6132
https://doi.org/10.1007/s00216-020-02655-z

REVIEW

Nanoelectrochemistry in the study of single-cell signaling

Ran Chen[1] · Kristen Alanis[1] · Theresa M. Welle[1] · Mei Shen[1]

Received: 15 February 2020 / Revised: 2 April 2020 / Accepted: 8 April 2020 / Published online: 18 May 2020

Abstract

Label-free biosensing has been the dream of scientists and biotechnologists as reported by Vollmer and Arnold (Nat Methods 5:591–596, 2008). The ability of examining living cells is crucial to cell biology as noted by Fang (Int J Electrochem 2011:460850, 2011). Chemical measurement with electrodes is label-free and has demonstrated capability of studying living cells. In recent years, nanoelectrodes of different functionality have been developed. These nanometer-sized electrodes, coupled with scanning electrochemical microscopy (SECM), have further enabled nanometer spatial resolution study in aqueous environments. Developments in the field of nanoelectrochemistry have allowed measurement of signaling species at single cells, contributing to better understanding of cell biology. Leading studies using nanoelectrochemistry of a variety of cellular signaling molecules, including redox-active neurotransmitter (e.g., dopamine), non-redox-active neurotransmitter (e.g., acetylcholine), reactive oxygen species (ROS), and reactive nitrogen species (RNS), are reviewed here.

Keywords Nanoelectrochemistry · Single cell · Neurotransmitters · ROS/RNS · Nanoelectrode

Introduction

Nanoelectrochemistry plays critical roles in a broad range of interdisciplinary research, spanning biochemistry, neuroscience, catalysis, molecular electronics, nanoscience (e.g., nanopores, nanobubbles, and nanoparticles), polymer science, electrodeposition, and renewable technologies [1–12]. Conducting chemical measurements in solution with nanometer spatial resolution, high temporal resolution, and ultra-high sensitivity and selectivity has been achieved with the recent advancements in nanoelectrochemistry. For example, nano-resolved scanning electrochemical microscopy (SECM) [13–15] has been successfully used in the high-resolution imaging of ion transport through single nanopores [16, 17], where non-resolution imaging was achieved by scanning a 17-nm radius nanoelectrode at a distance as low as 1.3 nm from a highly porous silicon membrane (Fig. 1a) [16]. Catalytic properties of the single individual nanoparticles have also been studied using nano-resolved SECM and nanoelectrodes with nanometer resolution (Fig. 1b, c) [18–23]. Nanoelectrochemistry with single molecule sensitivity has also been demonstrated [24–42]. Single hydrogen nanobubble nucleation has been studied on Pt nanoelectrodes and the critical nucleus size of stable nanobubbles has been analyzed [43–48]. Nanometric field-effect transistor devices have been developed to detect pH change in the extracellular microenvironment of living cells and have been employed to detect the adenosine-5′-triphosphate (ATP) release concentration based on stoichiometry [49]. The surface ion conductance and surface charge on single cells [50–53] have also been measured with nanoprobes coupled with scanning ion conductance microscopy [54]. Additionally, nanoelectrodes have been employed in the study of single nanoparticle collisions [55–59].

In addition to the above-mentioned advancements, signaling molecules/species secreted from the single living cells have been studied with nanoelectroanalytical methods, demonstrating the critical roles that nanoelectrochemistry plays in biology and neuroscience. We present below recent developments in nanoelectrochemistry which have enabled measurements of various signaling molecules including neurotransmitters (redox active and non-redox active) and reactive oxygen/nitrogen species at single living cells from a variety of cell types. Measuring these biochemical parameters at single cells is indispensable for understanding biology [60].

Published in the topical collection featuring *Female Role Models in Analytical Chemistry*.

✉ Mei Shen
mshen233@illinois.edu

[1] Department of Chemistry, University of Illinois at Urbana-Champaign, 600 South Mathews Avenue, Urbana, IL 61801, USA

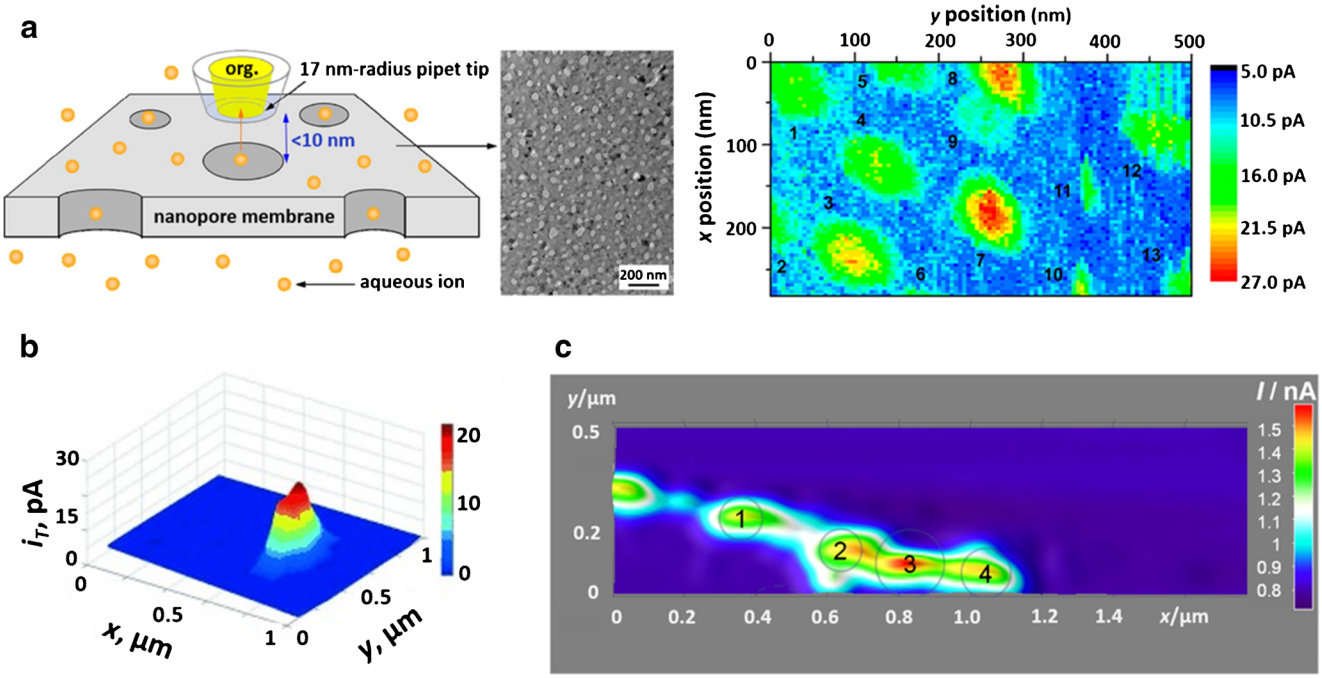

Fig. 1 **a** *Left*: Scheme of the nano-resolution imaging experiment, where a 17-nm nanoITIES electrode was positioned < 10 nm (as close as 1.3 nm) from the porous Si membrane (middle, transmission electron microscope (TEM) image). *Right*: Nano-resolution image of a highly porous Si membrane obtained with a nanoscale interface between two immiscible electrolyte solutions (nanoITIES) electrode (radius = 17 nm) and scanning electrochemical microscopy based on the ion flux across the nanopores. Reproduced or modified from ref. [16] with permission; copyright (2012) American Chemical Society. **b** SECM imaging of the hydrogen evolution reaction at an Au nanoparticle on a HOPG/polyphenylene substrate obtained with a 15-nm-radius Pt tip, reproduced or modified from ref. [18] with permission; copyright (2014) Wiley-VCH. **c** SECM image of H^+/H electron transfer reaction at Pt nanoparticles in 2 mM $HClO_4$ and 10 mM $NaClO_4$ measured by a Pt nanoelectrode with ~ 100-nm radius, reproduced or modified from ref. [19] with permission; copyright (2016) American Chemical Society

Recent advancements in the study of signaling molecules with nanoelectrochemistry

Neurotransmitters (redox active and non-redox active)

Neurotransmitters are the chemical messengers released during brain communication. Chemical sensing with electrodes offers chemical identity, quantification, and spatiotemporal information about biological processes in vivo [61]. Measuring transmitters using microelectrodes has generated key information on neuronal communication, contributing to our understanding of brain disorders, such as depression and addiction [62–80]. Recently, nanometer-sized carbon fiber [81–87] and nano-interface between two immiscible electrolyte solutions (ITIES) electrodes [88] have been developed to study neurotransmitter signaling in living neurons. We first review below leading studies on using nanocarbon electrodes to study redox-active transmitter signaling at the single living cells. Then, we present our recent work on high spatiotemporal study of acetylcholine (non-redox active) somatic exocytosis using nano-ITIES electrodes.

Redox-active neurotransmitters: Catecholamine

Catecholamines are important redox-active neurotransmitters in neuronal communication. Recent development of nanometer-sized carbon fiber electrodes enables the study of catecholamine release from single cells [81, 82, 84, 85] and dopamine release from fruit fly *Drosophila* larvae [83].

Using pharmacology and voltammetry measurements, Ewing's group has confirmed that PC12 cells release catecholamine, most likely dopamine [89]. Recently, they used nanotip conical carbon fiber microelectrodes for the intracellular detection of redox-active catecholamine released in living PC12 cells [81]. SEM images of the electrode are shown in Fig. 2a, b, where a diameter of 50–100 nm at the nanotip and total length of 30–100 µm were observed. When the nanotip of the electrode was strongly pressed against the PC12 soma membrane but without breaking into the cytosol, no amperometric signal was observed when no chemical stimulation was applied, showing that unstimulated exocytosis of catecholamine does not occur (Fig. 2d). However, when the electrode was penetrated through the cell membrane as indicated in Fig. 2c, even without any chemical stimulation, well-defined amperometric spikes were recorded (Fig. 2e). The same intracellular recording experiments were carried out in Ca^{2+}-free

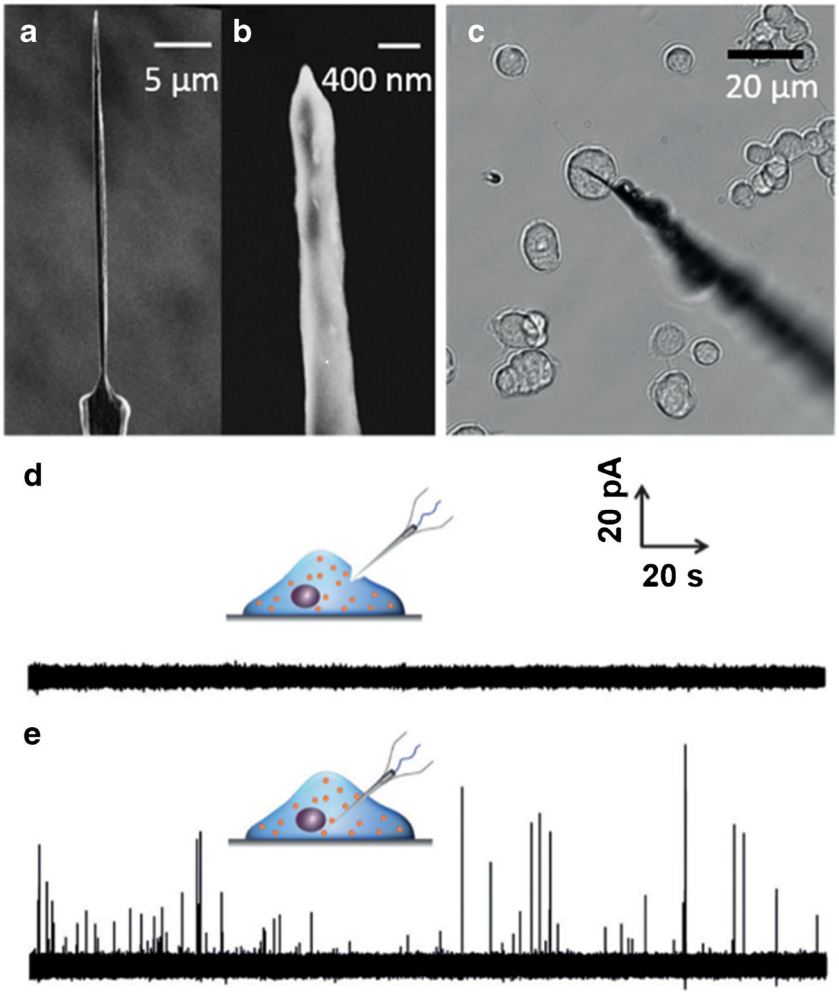

Fig. 2 **a** The global view of a nanotip conical carbon fiber microelectrode by scanning electron microscopy (SEM) (scale bar, 5 μm). The total length of the protruded carbon fiber was 30–100 μm. **b** The amplified view of the tip of a nanotip conical carbon fiber microelectrode by SEM (scale bar, 400 nm). The diameter of the nanotip was 50–100 nm. **c** Bright-field photomicrograph of a nanotip conical carbon fiber microelectrode placed in the cytoplasm of a single PC12 cell. **d** Amperometric trace of a nanotip conical carbon fiber microelectrode pushed against the cell membrane of a PC12 cell without breaking into the cytoplasm. **e** Amperometric trace of a nanotip conical carbon fiber microelectrode inside a PC12 cell. Rreproduced or modified from ref. [81] with permission; copyright (2015) Wiley-VCH

physiological saline, and no significant difference in the shape or the amount of catecholamine detected was observed. The authors suggested that the amperometric transients in Fig. 2e are from the adsorption, subsequent rupture, and expelling of the vesicle contents (mainly catecholamines, such as norepinephrine, epinephrine, and dopamine) at the electrode surface inside the cell.

Non-redox active: Acetylcholine (ACh)

Besides measuring redox-active neurotransmitters using nanocarbon fiber electrodes as presented above, further development on nanoelectrochemistry has also been made to enable the study of non-redox-active neurotransmitter, e.g., acetylcholine. While the redox-active transmitters, mainly dopamine, can be detected using carbon fiber nanoelectrodes based on electron transfer reaction, non-redox-active transmitters, on the other hand, cannot be detected directly on the carbon electrodes [69]. Although micrometer-sized enzyme-modified electrodes have been reported, they have been mainly used for the electrochemical detection of ACh in brain or brain slice [71, 90–95]. Our work expands further the toolbox of electrochemistry for the study of ACh neurotransmission from single neurons and single synapses with high spatiotemporal resolution and fast response time [61, 88]. We recently developed nanometer-sized electrodes for the detection of non-redox-active transmitters such as acetylcholine [96] and gamma-aminobutyric acid (GABA) [97], where the detection is based on the ion transfer across the interface between two immiscible electrolyte solutions (ITIES) [16, 17, 98–106]. This interface is formed between an organic electrolyte filling solution contained inside a nanopipet and an outside aqueous medium. The potential-driven transfer of ions across this interface generates a current [107]. The theory for chemical sensing with ITIES electrodes (a very broad field) is well established and the applied potential, $\Delta_o^w\phi$, follows the Nernst equation:

$$\Delta_o^w\phi = \Delta_o^w\phi_i^0 + \frac{RT}{Z_iF}\ln\left(\frac{a_i^o}{a_i^w}\right)$$

where $\Delta_o^w\phi^0$ is the standard ion transfer potential, R is the gas constant, T is the temperature, z_i is the charge of the ion (i), F is the Faraday constant, and a_i^o and a_i^w are the activity of the

ionic analyte in the organic and aqueous phase, respectively. The standard ion transfer potential is related to the Gibbs free energy of transfer, which is a function of the structure and hydrophilicity of each analyte; thus, analytes can be identified using ITIES electrodes. The mass transfer limiting current measured at nanoITIES electrodes is a function of the concentration of the analyte, which can thus be used for the quantification of the neurotransmitters [107]. This quantitative detection of ACh is demonstrated in Fig. 3a, where a linear increase in the current was observed while we increased the concentration of ACh from 0.25 to 6 mM [96]. The limit of detection depends on the size of ITIES electrodes. For instance, LOD of 26 μM was measured for ACh detection for a nanoITIES electrode of ~ 210 nm in radius [88]. We have also performed in vitro control experiments to verify the selectivity of the nanoITIES electrode for ACh detection against other substances that have been identified or suggested to be released from the neuronal model, pedal ganglion neurons of *Aplysia californica* (Fig. 3b) [61]. We further demonstrated high spatiotemporal study of ACh signaling from single living *Aplysia* neurons (somatic exocytosis [88] and synaptic cleft chemical transmission [61]) using a nano-resolved scanning electrochemical microscope (SECM) and nanoITIES electrode.

In our study of non-redox-active transmitter signaling from single neuron cells, SECM with 0.3-nm step size was used to enable the accurate positioning of the nanoITIES electrodes to be ~ 140 nm away (determined from the SECM approach curve) from the release sites on the soma. Once positioned at nanometer distance from the soma with SECM, we employed amperometry to study the release of ACh in response to high-concentration K^+ stimulation, to learn about its concentration and dynamics with a time resolution on the order of milliseconds. In situ release of ACh (Fig. 4a) measured with a signal to noise ratio of 6–19 was observed on the ITIES electrodes with radii of 750 to 860 nm. Key information related to cellular communication was determined, including extracellular concentration of acetylcholine during somatic exocytosis to be 2.7 (± 1.0) μM calculated from peak current, the number of molecules released to be 4.8 (± 1.3) × 10^7, the dynamics of exocytosis, vesicle density (Fig. 4b), Ca^{2+} dependence on somatic exocytosis (Fig. 4c, d), and the effect of electrode-release site distance on the measured signal (Fig. 4e, f).

Our study shows that nanometer resolution positioning of the neurotransmitter sensing probe to be nanometer distance away from neurons has advantages of high signal to noise measurements. When the nanoelectrode is nanometer distance

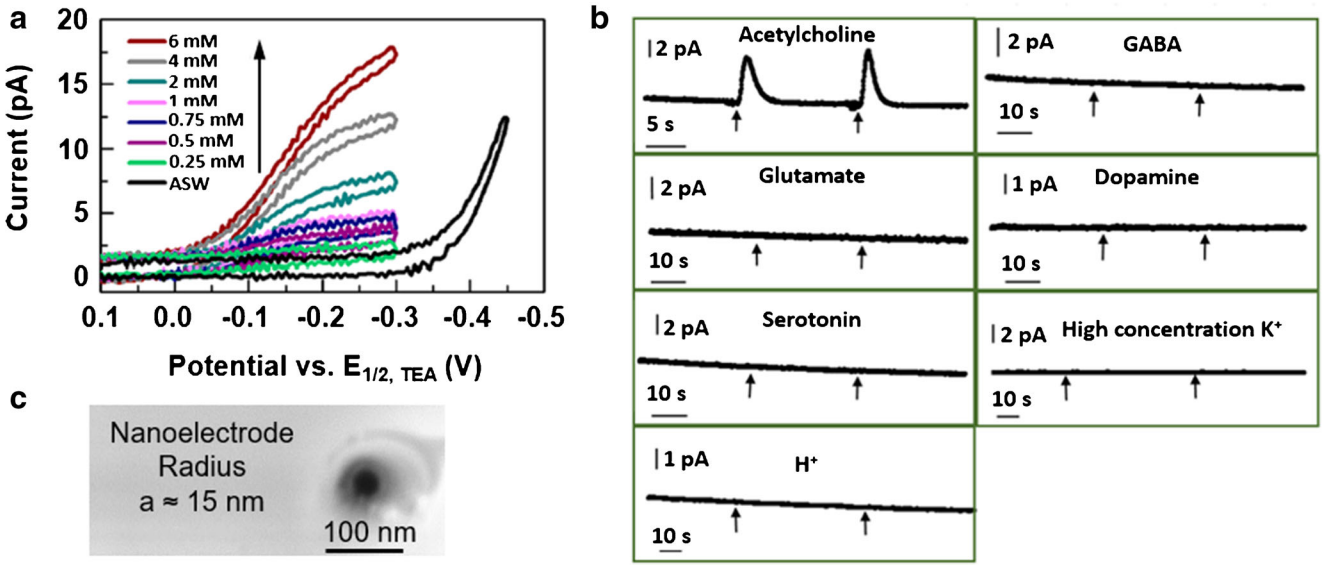

Fig. 3 Characterization of nanoITIES electrodes for the selective detection of acetylcholine (ACh). **a** Cyclic voltammograms of 0.25–6 mM ACh using a nanoITIES electrode with a radius of ~7 nm. Tetraethylammonium (TEA) was added to the aqueous phase and potential of ACh detection was reported with respect to the half wave transfer potential of TEA, $E_{1/2,\ TEA}$. Reproduced or modified from ref. [96] with permission; copyright (2015) American Chemical Society. **b** In vitro test of the selectivity for ACh detection against possible interfering species on the nanoITIES electrodes. Possible transmitters known to be released from the pedal ganglion neuron of *Aplysia californica*, the high concentration of K^+ used in the stimulation solution, and pH variance accompanying exocytosis were tested for selectivity via flow injecting each of the species while monitoring the current-time trace. Appearance of current peaks indicates the electrode's selectivity for acetylcholine detection. Lack of signal for gamma-aminobutyric acid (GABA), glutamate, dopamine, serotonin, and high-concentration K^+ and H^+ verifies that these species do not generate an interfering current. Applied potential is the diffusion limiting potential of ACh detection, $E_{ACh} = -0.48$ V vs. $E_{1/2,\ TBA}$, which was used in the amperometric detection of ACh released from living neuronal structures in real time. Reproduced or modified from ref. [61] with permission; copyright (2019) American Chemical Society. **c** High-resolution scanning electron microscope (SEM) picture of a nanoITIES electrode with radius of ~ 15 nm from Shen lab. Reproduced or modified from ref. [61] with permission; copyright (2019) American Chemical Society

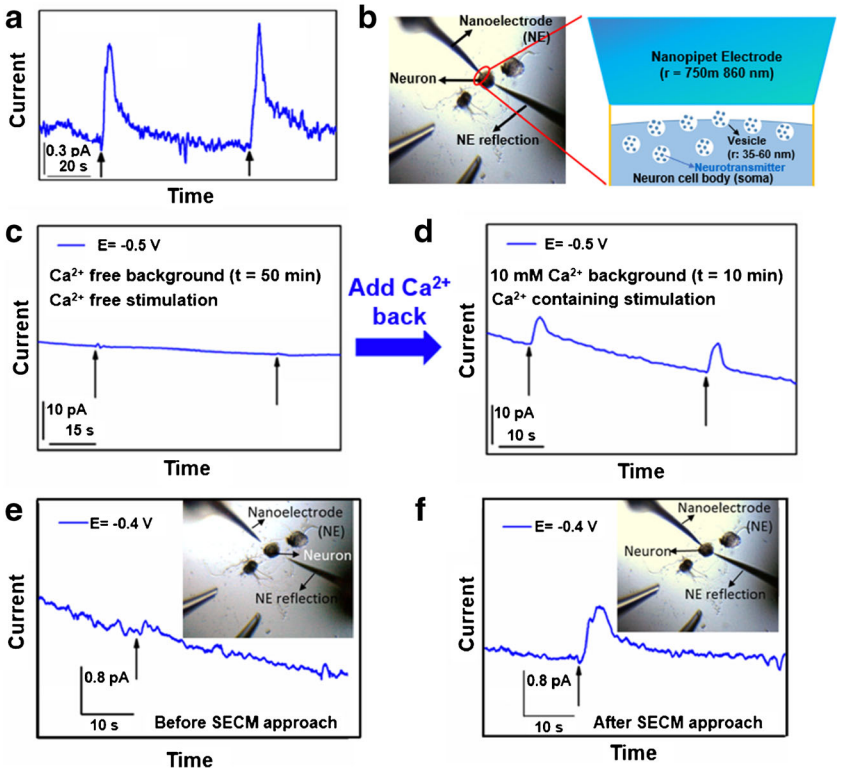

Fig. 4 Nano-resolved study of somatic cholinergic transmitter signaling of *Aplysia* neurons achieved with nanoITIES electrodes and scanning electrochemical microscopy. **a** Amperometric recordings of ACh release from single *Aplysia* neuron in response to high-concentration K^+ stimulation, indicated by the arrows. **b** The optical image of the nanoelectrode positioned at ~140 nm away from the neuron (left). Number of vesicles per unit area was measured using in vivo amperometry with the scheme of the vesicles under the nanoelectrode shown on the right. The measured vesicle density is $\sim 25 \pm 2$ vesicles/μm^2. **c** ACh release in response to Ca^{2+}-free high-concentration K^+ chemical stimulation, measured at 50 min after replacing standard cellular medium with Ca^{2+}-free cellular medium. **d** ACh release from cell in response to Ca^{2+}-containing high-concentration K^+ chemical stimulation, 10 min after adding 10 mM Ca^{2+} back to stimulation solution and cellular medium. Amperometric *i-t* curve in (**e**) shows no significant response detected upon stimulation prior to SECM approach curve where the electrode was several micrometers away. In contrast, well-defined peak response (**f**) was recorded upon stimulation after performing SECM approach. Insets are optical microscopic pictures of the nanoelectrodes and neurons. Applied potential is the diffusion-limited potential for acetylcholine detection. Nanoelectrode radii are 780–860 nm. Application of chemical stimulation was indicated by black arrows. Reproduced or modified from ref. [88] with permission; copyright (2018) Royal Chemical Society

from neuron surface, transmitter release dynamics were successfully measured with high signal to noise ratio (Fig. 4f). In contrast, without SECM nanopositioning, when the nanoelectrode is several micrometers away from the cell surface, a much lower signal to noise ratio was observed (Fig. 4e). Our results show that it is advantageous to use SECM to position nanoelectrode to be nanometer away from cell surface to interrogate the dynamics of signaling molecules.

Our work further demonstrated nanoITIES electrodes are powerful to probe the mechanism of cellular signaling. It is unknown how ACh is released from *Aplysia californica*. We performed a Ca^{2+} dependence study using nanoITIES electrodes, since Ca^{2+} is known to be involved in the vesicular release of transmitters [108]. When Ca^{2+} was not present, no exocytosis events were observed in response to high-concentration K^+ stimulation (Fig. 4c); in contrast, acetylcholine exocytosis events recovered once Ca^{2+} had been added back (Fig. 4d). Our findings suggest the vesicular release pathway of acetylcholine somatic exocytosis from *Aplysia*.

Finally, our work demonstrated unprecedentedly that in vivo amperometry is a powerful versatile technique to measure number of vesicles per unit area, while collecting signaling dynamics in real time. For instance, analysis of the half peak width and number of molecules suggests the measurement of multiple vesicular contents released from the single neuron soma via nanoITIES electrodes with radii of 750–860 nm during each peak event [88]. Using the content per vesicle as suggested in our recent single synaptic study of acetylcholine release from the same animal model [61], we calculated the releasable vesicle density to be 25 ± 2 vesicles/μm^2 (Fig. 4b). This number is in similar order of magnitude to the value of 90 vesicles/μm^2 observed in a recent study using 3D reconstruction of synaptic boutons from serial transmission electron microscopy sections [109].

In summary, our research has expanded the capability of in vivo amperometry to measure in real time the signaling dynamics of non-redox-active transmitters besides redox-active transmitters. Our work also demonstrated nanoelectrochemistry

is an emerging method to measure number of vesicles/unit area in living cell conditions, where quantitative information and dynamics of signaling molecules can also be measured.

ROS/RNS

Reactive oxygen and nitrogen species (ROS and RNS), including radicals, such as $O_2^{\cdot-}$, $OH^{\cdot}$, $NO^{\cdot}$, and $NO_2^{\cdot}$, and non-radicals, such as ONO_2^-, H_2O_2, and HOCl, are reported to serve as molecular signals activating stress responses that are beneficial to an organism; they also have been shown to modulate numerous biochemical processes, including glucose uptake, gene expression, and calcium signaling [110–116]. However, overproduction of ROS/RNS can overwhelm cellular radical-scavenging and repairing systems, causing tissue dysfunction and oxidative stress [114, 117]. Oxidative stress is further related to cardiovascular and neurodegenerative diseases [118, 119]. ROS/RNS concentration in the cell is also an important carcinogenic factor because tumor progression is associated with high levels of ROS/RNS, and further concentration increases in these species can overwhelm the antioxidant capacity of the cell and cause the death of the cell [120]. Considering above, it is critical to detect ROS/RNS, and a lot of study has been carried out using microelectrodes [121–124], but very few using nanoelectrodes [122]. Recently, studying ROS/RNS using nanoelectrochemistry has been a growing area of interest. We present below the leading studies where nanoelectrodes were employed in the measurements of ROS and RNS. Nanoelectrodes are especially advantageous for the intracellular measurement of these species due to their small sizes, which can minimize the damage during penetration of the living cell.

Mirkin, Amatore et al. developed platinized carbon nanoelectrodes with well-characterized geometry and used them as scanning electrochemical microscopy (SECM) tips to measure ROS/RNS inside non-cancerous and metastatic human breast cells [125]. The oxidation of some ROS/RNS (e.g., hydrogen peroxide) was difficult on carbon surfaces; however, hydrogen peroxide could be easily and quantitatively detected on platinum black or platinized electrodes [68, 123, 124, 126–128]. The carbon nanoelectrodes were produced by chemical vapor deposition (CVD) in pulled nanopipettes, and the CVD conditions were adjusted so that carbon completely blocked the pipette channel except for a small cavity adjacent to the pipette orifice (Fig. 5a). The surface of the nanocavity was first activated electrochemically by sweeping the carbon electrode potential (between 200 and − 400 mV vs. Ag/AgCl) in a platinization solution (containing 0.15% H_2PtCl_6) followed by the deposition of Pt black electrochemically to generate the platinized carbon nanoelectrode (Fig. 5b).Then, the authors used SECM approach curves to position the nanoelectrode inside the cell.

The authors further used the platinized carbon nanoelectrode to detect intracellular ROS/RNS in living cells (Fig. 5c), where voltammograms obtained inside the metastatic breast cancer cells showed high oxidation current, while the current measured from non-cancerous cells remains almost indistinguishable from the background. To quantify the concentration of each species of ROS/RNS (including H_2O_2, ONO_2^-, $NO^{\cdot}$, and $NO_2^{\cdot}$), the authors measured the normalized oxidation voltammograms of H_2O_2, ONO_2^-, $NO^{\cdot}$, and $NO_2^{\cdot}$ (Fig. 5d), and the optimal detection potentials for each species were selected (indicated by the dashed lines in Fig. 5d). For example, when the nanoelectrode is biased at 300 mV, the current only corresponded to the oxidation of H_2O_2, and its concentration can be obtained. At 450 mV, mainly the oxidation of both H_2O_2 and ONO_2^- occurs. Since H_2O_2 concentration has been obtained from the oxidation current at 300 mV, the current corresponding to ONO_2^- oxidation can be further calculated from the current measured at 450 mV minus the current contribution from H_2O_2. Similar calculations are carried out at 620 mV and 850 mV to extract the concentration of $NO^{\cdot}$, and $NO_2^{\cdot}$.

For intracellular study, the authors collected the current trace versus time at 300 mV (blue), 450 mV (orange), 620 mV (gray), and 850 mV (yellow) upon penetrating the nanoelectrode into the cancerous cell (Fig. 5e), and then deduced the concentration trace of H_2O_2 (blue), ONO_2^- (orange), $NO^{\cdot}$ (gray), and $NO_2^{\cdot}$ (yellow) versus time (Fig. 5f) using diffusion coefficients of 1.5×10^{-5} cm^2/s for all species [129]. The authors concluded that platinized nanoelectrodes are a suitable analytical platform for studying ROS/RNS-related carcinogenesis and are potentially useful for early diagnostics of aggressive human breast tumors. Cell viability in SECM penetration experiments and the effect of tip size on the cell viability was studied as well. The authors observed that the integrity of the membrane and cell viability maintained when cells were penetrated by the 20-nm and 150-nm radius tips, while the cell was damaged when penetrated by a 600-nm radius tip.

Amatore, Huang et al. recently reported the fabrication of a nanowire electrode (NWE) that consists of a silicon carbide core (SiC) coated with carbon (Fig. 6a), which was further platinized to measure ROS/RNS inside macrophages (Fig. 6b) [130]. Macrophages are responsible for the phagocytosis of cell debris and pathogens that they digest by the release of large amounts of ROS and RNS inside the phagolysosome [68, 131]. The SiC nano-core was used to provide mechanical strength. Platinization was carried out in 0.5-mM H_2PtCl_6 solutions under microscopic control. These SiC@C NWEs have the diameter of 300–500 nm and ~ 5 μm in length (estimated from Fig. 6a). The authors inserted the platinized SiC@C NWEs into the Hela cells using a micromanipulator, and performed viability tests and electrochemical measurements to confirm that membranes tightly seal

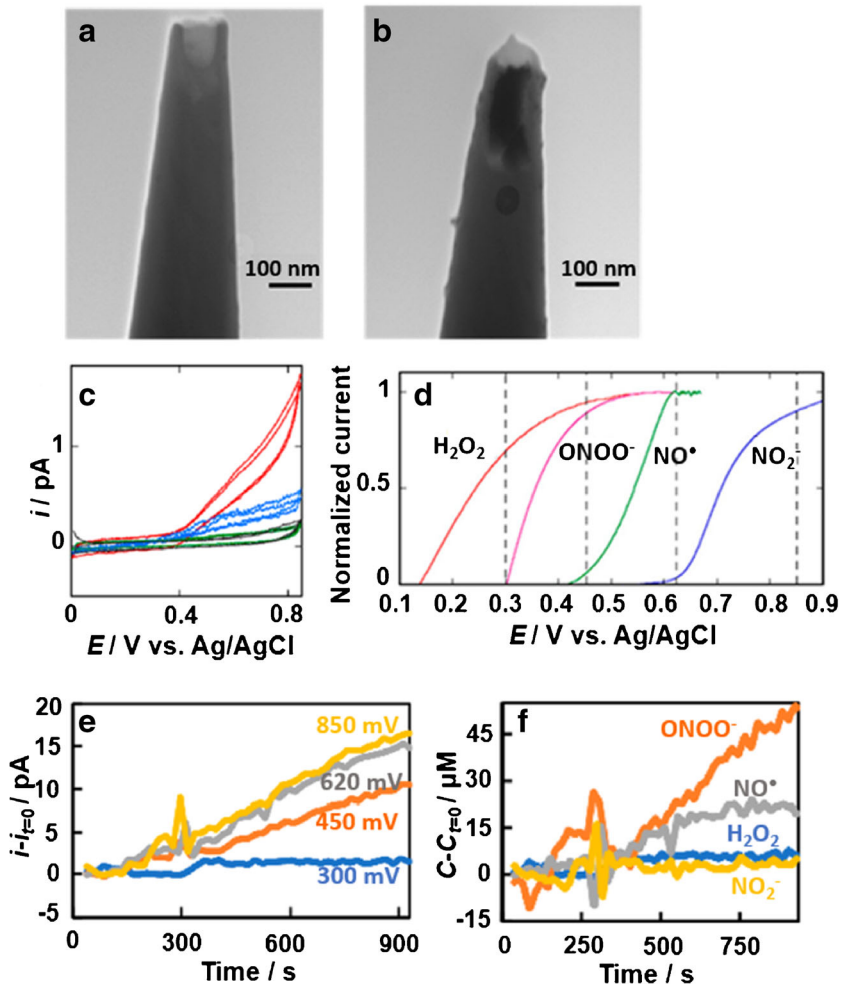

Fig. 5 **a** TEM image of the carbon-filled pipette before platinization (scale bar, 100 nm). **b** TEM image of the carbon-filled pipette after platinization (scale bar, 100 nm). **c** The voltammogram recorded inside non-cancerous breast cells (green) and metastatic breast cancer cells (blue and red) compared with the extracellular buffer background (black). The black curve overlapped with the green curve. **d** Normalized oxidation voltammograms of the ROS/RNS. Voltammograms were taken by different platinized nanoelectrodes with around 100-nm radius and normalized against their plateau currents. Vertical dashed lines indicate optimal detection potential for each species. **e** Traces of tip current versus time at different potentials measured inside a metastatic breast cancer cell by quadruple potential-pulse chronoamperometry. Tip potentials are 300 (blue), 450 (orange), 620 (gray), and 850 (yellow) mV. Tip radius was 300 nm. $t = 0$ is the moment when the tip was inserted into the cell. **f** Traces of concentration of H_2O_2 (blue), $ONOO^-$ (orange), $NO^{\cdot}$ (gray), and NO_2^- (yellow) versus time as deduced from the current shown in (**e**) and reported relative to their concentration at $t = 0$. Reproduced or modified from ref. [125] with permission; copyright (2017) American Chemical Society

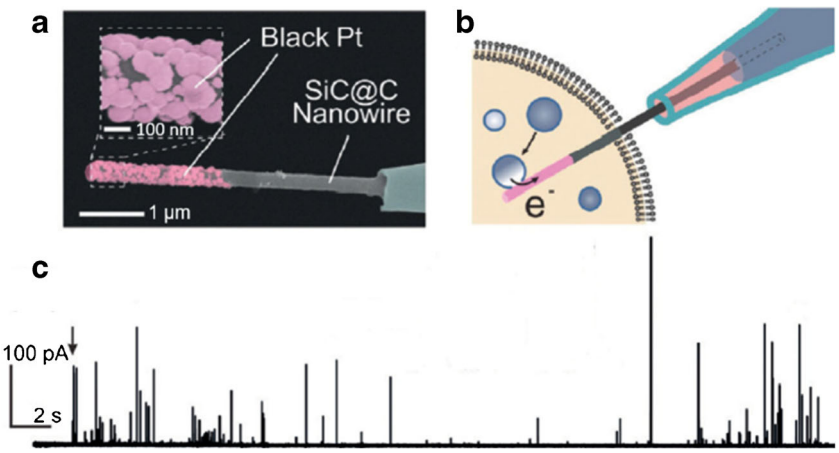

Fig. 6 **a** SEM image of a platinized SiC@C NWE. Inset: A magnified SEM image of its tip. **b** Schematic of a platinized SiC@C NWE inserted into a macrophage with a phagolysosome bursting onto it. **c** Amperometric traces recorded after insertion of a platinized SiC@C NWE into a macrophage; the arrow indicates the moment of insertion. Reproduced or modified from ref. [130] with permission; copyright (2017) Wiley-VCH

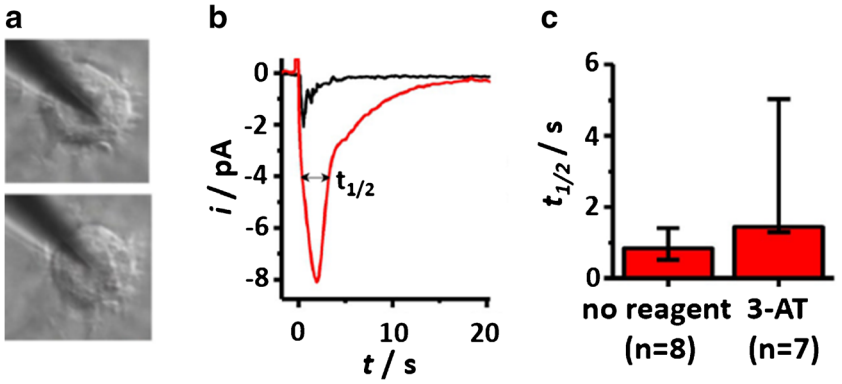

Fig. 7 **a** Optical micrographs of a PB-modified CNE inserted into a murine macrophage (top) and after retraction (bottom). **b** Comparison of the current responses for untreated cells (black) and after addition of 20 mM 3-AT to inhibit catalase (red). **c** Comparison of cathodic peak half-life between catalase-inhibited and non-treated cells. Column heights represent the median, whereas whiskers show the 25th and 75th percentiles. Reproduced or modified from ref. [136] with permission; copyright (2016) Wiley-VCH

around NWE shaft. $Ru(NH_3)_6^{3+}$ was added into the cellular medium as it could not cross the intact cell membrane, and the authors monitored the voltammogram of $Ru(NH_3)_6^{3+}$ reduction as the NWEs penetrated into the cell. The authors observed that the current for $Ru(NH_3)_6^{3+}$ reduction decreased as the electrode penetrated deeper and deeper into the cell, thus confirmed a tight seal was formed around the NWE shaft. They further performed measurements of ROS/RNS in individual macrophages after inserting platinized tips of SiC@C NWEs inside macrophages of ~ 10 μm in diameter. A large series of transient current spikes were recorded superimposed onto a zero-current baseline (Fig. 6c), and no current spikes were observed when the applied electrode potential was too low to oxidize ROS/RNS. The current spikes were suggested to represent the detection of ROS/RNS expelled by the phagolysosomes bursting onto the platinized surface of the inserted NWEs, consistent with recent studies that lipid vesicles would break apart and rapidly expel its cargo after coming into contact with an electrode [81, 132–134]. Recently, the platinized SiC@C NWE has been used to monitor ROS in HepG2 cancer cells (human hepatoma cells) as well [135].

Schuhmann et al. recently developed a carbon nanoelectrode modified with Prussian Blue (PB) for the quantification of H_2O_2 at the single-cell level [136, 137]. PB is an electrocatalyst for the reduction of H_2O_2. The PB-modified carbon nanoelectrode (CNE) with radius between 50 and 200 nm was inserted into murine macrophages to study the impact of cell penetration on viability of the cell and ROS production. The optical micrographs of a macrophage with a PB-modified CNE inserted and after CNE retraction showed that the cell maintained its shape (top and bottom figure in Fig. 7a, respectively) and the authors concluded that a CNE does not impact cell viability. The authors observed a cathodic amperometric current spike (in the negative direction) after successful penetration of the CNE into the membrane and suggested these sharp cathodic current spikes are likely caused by oxidative outbursts induced by the insertion of CNE. As a control, bare CNEs without PB modification were inserted into cells and no current signal was observed upon penetration. The authors further studied the effect of 3-amino-1,2,4-triazole (3-AT) treatment on the intracellular H_2O_2. 3-AT deactivates catalase; catalase accelerates the disproportionation of H_2O_2 in the cell, and deactivating catalase with 3-AT leads to an accumulation of H_2O_2 in the cell. This effect was confirmed (Fig. 7b), where the cathodic peak of 3-AT-treated cells showed a slower decay upon cell penetration, with substantially longer half-lives (Fig. 7c). The authors concluded that PB-modified CNEs are suitable for H_2O_2 detection.

Conclusion and outlook

Nanoelectrochemistry for the investigation of single-cell signaling is a significant and growing area of research that invites further study. While this review is about signaling molecules, a variety of other cellular functions and properties have been characterized using nanoelectrochemistry, including cellular volume regulation [138], cellular permeability and ion transport [139, 140], surface charge [51, 52, 141], ion conductance [50, 53], and oxygen concentration [142, 143]. Developing new electrodes with even smaller sizes, different functionality, and geometry certainly will expand the fields further, enabling tackling challenges and answering intriguing questions in new ways. We look forward to lots of exciting advancements in the field of nanoelectrochemistry in the 2nd decade of the twenty-first century.

Funding information The authors appreciate the financial support from the National Science Foundation with a CAREER award (CHE 19-45274) to M.S. as well as the support from University of Illinois at Urbana-Champaign.

Compliance with ethical standards

Conflict of interest The authors declare that they have no conflict of interest.

Research involving human participants and/or animals This article does not involve any human participant or animals.

References

1. Mirkin MV, Amemiya S. Nanoelectrochemistry. Boca Raton: CRC Press; 2014.
2. Barton ZJ, Rodríguez-López J. Lithium ion quantification using mercury amalgams as in situ electrochemical probes in nonaqueous media. Anal Chem. 2014;86(21):10660–7.
3. Burgess M, Moore JS, Rodríguez-López J. Redox active polymers as soluble nanomaterials for energy storage. Acc Chem Res. 2016;49(11):2649–57.
4. Murray RW. Nanoelectrochemistry: metal nanoparticles, nanoelectrodes, and nanopores. Chem Rev. 2008;108(7):2688–720.
5. Rassaei L, Singh PS, Lemay SG. Lithography-based nanoelectrochemistry. Anal Chem. 2011;83(11):3974–80.
6. Cox JT, Zhang B. Nanoelectrodes: recent advances and new directions. Annu Rev Anal Chem. 2012;5:253–72.
7. Fan Y, Han C, Zhang B. Recent advances in development and application of nanoelectrodes. Analyst. 2016;141(19):5474–87.
8. Clausmeyer J, Schuhmann W. Nanoelectrodes: applications in electrocatalysis, single-cell analysis and high-resolution electrochemical imaging. Trends Anal Chem. 2016;79:46–59.
9. Edwards MA, Robinson DA, Ren H, Cheyne CG, Tan CS, White HS. Nanoscale electrochemical kinetics & dynamics: the challenges and opportunities of single-entity measurements. Faraday Discuss. 2018;210:9–28.
10. Goines S, Dick JE. Review-electrochemistry's potential to reach the ultimate sensitivity in measurement science. J Electrochem Soc. 2020;167:037505.
11. Ying YL, Ding Z, Zhan D, Long YT. Advanced electroanalytical chemistry at nanoelectrodes. Chem Sci. 2017;8:3338–48.
12. Huang K, Clausmeyer J, Luo L, Jarvis K, Crooks RM. Shape-controlled electrodeposition of single Pt nanocrystals onto carbon nanoelectrodes. Faraday Discuss. 2018;210:267–80.
13. Bard AJ, Fan F-RF, Kwak J, Lev O. Scanning electrochemical microscopy introduction and principles. Anal Chem. 1989;61(2):132–8.
14. Bard AJ, Fan F-RF, Pierce DT, Unwin PR, Wipf DO, Zhou F. Chemical imaging of surfaces with the scanning electrochemical microscope. Science. 1991;254(5028):68–74.
15. Kai T, Zoski CG, Bard AJ. Scanning electrochemical microscopy at the nanometer level. Chem Commun. 2018;54:1934–47.
16. Shen M, Ishimatsu R, Kim J, Amemiya S. Quantitative imaging of ion transport through single nanopores by high-resolution scanning electrochemical microscopy. J Am Chem Soc. 2012;134(24):9856–9.
17. Chen R, Balla RJ, Lima A, Amemiya S. Characterization of nanopipet-supported ITIES tips for scanning electrochemical microscopy of single solid-state nanopores. Anal Chem. 2017;89(18):9946–52.
18. Sun T, Yu Y, Zacher BJ, Mirkin MV. Scanning electrochemical microscopy of individual catalytic nanoparticles. Angew Chem Int Ed. 2014;53(51):14120–3.
19. Kim J, Renault C, Nioradze N, Arroyo-Currás N, Leonard KC, Bard AJ. Electrocatalytic activity of individual Pt nanoparticles studied by nanoscale scanning electrochemical microscopy. J Am Chem Soc. 2016;138(27):8560–8.
20. Kim J, Dick JE, Bard AJ. Advanced electrochemistry of individual metal clusters electrodeposited atom by atom to nanometer by nanometer. Acc Chem Res. 2016;49(11):2587–95.
21. Mirkin MV, Sun T, Yu Y, Zhou M. Electrochemistry at one nanoparticle. Acc Chem Res. 2016;49(10):2328–35.
22. Oja SM, Robinson DA, Vitti NJ, Edwards MA, Liu Y, White HS, et al. Observation of multipeak collision behavior during the electro-oxidation of single Ag nanoparticles. J Am Chem Soc. 2017;139(2):708–18.
23. Anderson TJ, Zhang B. Single-nanoparticle electrochemistry through immobilization and collision. Acc Chem Res. 2016;49(11):2625–31.
24. Bard AJ, Fan F-RF. Electrochemical detection of single molecules. Acc Chem Res. 1996;29(12):572–8.
25. Mathwig K, Aartsma TJ, Canters GW, Lemay SG. Nanoscale methods for single-molecule electrochemistry. Annu Rev Anal Chem. 2014;7(1):383–404.
26. Lemay SG, Kang S, Mathwig K, Singh PS. Single-molecule electrochemistry: present status and outlook. Acc Chem Res. 2013;46(2):369–77.
27. Singh PS, Kätelhön E, Mathwig K, Wolfrum B, Lemay SG. Stochasticity in single-molecule nanoelectrochemistry: origins, consequences, and solutions. ACS Nano. 2012;6(11):9662–71.
28. Lu J, Fan Y, Howard MD, Vaughan JC, Zhang B. Single-molecule electrochemistry on a porous silica-coated electrode. J Am Chem Soc. 2017;139(8):2964–71.
29. Fan Y, Anderson TJ, Zhang B. Single-molecule electrochemistry: from redox cycling to single redox events. Curr Op Electrochem. 2018;7:81–6.
30. White RJ, Ervin EN, Yang T, Chen X, Daniel S, Cremer PS, et al. Single ion-channel recordings using glass nanopore membranes. J Am Chem Soc. 2007;129(38):11766–75.
31. Johnson RP, Fleming AM, Beuth LR, Burrows CJ, White HS. Base flipping within the α-hemolysin latch allows single-molecule identification of mismatches in DNA. J Am Chem Soc. 2016;138(2):594–603.
32. An N, Fleming AM, White HS, Burrows CJ. Nanopore detection of 8-oxoguanine in the human telomere repeat sequence. ACS Nano. 2015;9(4):4296–307.
33. Zhao J, Zaino LP III, Bohn PW. Potential-dependent single molecule blinking dynamics for flavin adenine dinucleotide covalently immobilized in zero-mode waveguide array of working electrodes. Faraday Discuss. 2013;164:57–69.
34. Han D, Crouch GM, Fu K, Zaino LP III, Bohn PW. Single-molecule spectroelectrochemical cross-correlation during redox cycling in recessed dual ring electrode zero-mode waveguides. Chem Sci. 2017;8:5345–55.
35. Pan S, Wang G. Single molecule and single event nanoelectrochemical analysis. In: Pierce DT, Zhao JX, editors. Trace analysis with nanomaterials. Weinheim: Wiley-VCH; 2010. p. 319–39.
36. Singh PS, Katelhon E, Mathwig K, Wolfrum B, Lemay SG. Stochasticity in single-molecule nanoelectrochemistry: origins, consequences, and solutions. ACS Nano. 2012;6(11):966–71.
37. Nichols RJ, Higgins SJ. Single molecule nanoelectrochemistry in electrical junctions. Acc Chem Res. 2016;49(11):2640–8.
38. Palacios RE, Fan FRF, Bard AJ, Barbara PF. Single-molecule spectrochemistry (SMS-EC). J Am Chem Soc. 2006;128(28):9028–9.
39. Hill CM, Clayton DA, Pan S. Combined optical and electrochemical methods for studying electrochemistry at the single molecule and single particle level: recent progress and perspectives. Phys Chem Chem Phys. 2013;15(48):20797–807.

40. Zaleski S, Wilson AJ, Mattei M, Chen X, Goubert G, Cardinal M, et al. Investigating nanoscale electrochemistry with surface- and tip- enhanced Raman spectroscopy. Acc Chem Res. 2016;49(9): 2023–30.
41. Fan F-RF, Bard AJ. Electrochemical detection of single molecules. Science. 1995;267(5199):871–4.
42. Ervin EN, Kawano R, White RJ, White HS. Simultaneous alternating and direct current readout of protein ion channel blocking events using glass nanopore membranes. Anal Chem. 2008;80(6): 2069–76.
43. Chen Q, Luo L, Faraji H, Feldberg SW, White HS. Electrochemical measurements of single H2 nanobubble nucleation and stability at Pt nanoelectrodes. J Phys Chem Lett. 2014;5(20):3539–44.
44. Chen Q, Luo L, White HS. Electrochemical generation of a hydrogen bubble at a recessed platinum nanopore electrode. Langmuir. 2015;31(15):4573–81.
45. Chen Q, Wiedenroth HS, German SR, White HS. Electrochemical nucleation of stable N2 nanobubbles at Pt nanoelectrodes. J Am Chem Soc. 2015;137(37):12064–9.
46. German SR, Edwards MA, Chen Q, Liu Y, Luo L, White HS. Electrochemistry of single nanobubbles. Estimating the critical size of bubble-forming nuclei for gas-evolving electrode reactions. Faraday Discuss. 2016;193:223–40.
47. Soto ÁM, German SR, Ren H, van der Meer D, Lohse D, Edwards MA, et al. The nucleation rate of single O2 nanobubbles at Pt nanoelectrodes. Langmuir. 2018;34(25):7309–18.
48. German SR, Edwards MA, Ren H, White HS. Critical nuclei size, rate, and activation energy of H2 gas nucleation. J Am Chem Soc. 2018;140(11):4047–53.
49. Zhang Y, Clausmeyer J, Babakinejad B, López Córdoba A, Ali T, Shevchuk A, et al. Spearhead nanometric field-effect transistor sensors for single-cell analysis. ACS Nano. 2016;10(3):3214–21.
50. Zhou L, Gong Y, Hou J, Baker LA. Quantitative visualization of nanoscale ion transport. Anal Chem. 2017;89(24):13603–9.
51. Perry D, Paulose Nadappuram B, Momotenko D, Voyias PD, Page A, Tripathi G, et al. Surface charge visualization at viable living cells. J Am Chem Soc. 2016;138(9):3152–60.
52. Zhu C, Zhou L, Choi M, Baker LA. Mapping surface charge of individual microdomains with scanning ion conductance microscopy. ChemElectroChem. 2018;5(20):2986–90.
53. Chen B, Perry D, Page A, Kang M, Unwin PR. Scanning ion conductance microscopy: quantitative nanopipette delivery-substrate electrode collection measurements and mapping. Anal Chem. 2019;91(3):2516–24.
54. Chen C-C, Zhou Y, Baker LA. Scanning ion conductance microscopy. Annu Rev Anal Chem. 2012;5(1):207–28.
55. Robinson DA, Liu Y, Edwards MA, Vitti NJ, Oja SM, Zhang B, et al. Collision dynamics during the electrooxidation of individual silver nanoparticles. J Am Chem Soc. 2017;139(46):16923–31.
56. Hao R, Fan Y, Zhang B. Imaging dynamic collision and oxidation of single silver nanoparticles at the electrode/solution interface. J Am Chem Soc. 2017;139(35):12274–82.
57. Zhang F, Edwards MA, Hao R, White HS, Zhang B. Collision and oxidation of silver nanoparticles on a gold nanoband electrode. J Phys Chem C. 2017;121(42):23564–73.
58. Li P, He Q, Liu HX, Liu Y, Su JJ, Tian N, et al. Collision incidents of single tetrahexahedral platinum nanocrystals recorded by a carbon nanoelectrode. ChemElectroChem. 2018;5(20):3068–72.
59. Pandey P, Garcia J, Guo J, Wang X, Yang D, He J. Differentiation of metallic and dielectric nanoparticles in solution by single-nanoparticle collision events at the nanoelectrode. Nanotechnology. 2019;31(1):015503.
60. Cluzel P, Surette M, Leibler S. An ultrasensitive bacterial motor revealed by monitoring signaling proteins in single cells. Science. 2000;287(5458):1652.
61. Shen M, Qu Z, DesLaurier J, Welle TM, Sweedler JV, Chen R. Single synaptic observation of cholinergic neurotransmission on living neurons: concentration and dynamics. J Am Chem Soc. 2018;140(25):7764–8.
62. Perry M, Li Q, Kennedy RT. Review of recent advances in analytical techniques for the determination of neurotransmitters. Anal Chim Acta. 2009;653(1):1–22.
63. Ge S, Koseoglu S, Haynes CL. Bioanalytical tools for single-cell study of exocytosis. Anal Bioanal Chem. 2010;397(8):3281–304.
64. Rogers ML, Boutelle MG. Real-time clinical monitoring of biomolecules. Annu Rev Anal Chem. 2013;6:427–53.
65. Schulte A, Nebel M, Schuhmann W. Scanning electrochemical microscopy in neuroscience. Annu Rev Anal Chem. 2010;3: 299–318.
66. Polcari D, Dauphin-Ducharme P, Mauzeroll J. Scanning electrochemical microscopy: a comprehensive review of experimental parameters from 1989 to 2015. Chem Rev. 2016;116(22): 13234–78.
67. Bergner S, Vatsyayan P, Matysik F-M. Recent advances in high resolution scanning electrochemical microscopy of living cells – a review. Anal Chim Acta. 2013;775:1–13.
68. Amatore C, Arbault S, Guille M, Lemaître F. Electrochemical monitoring of single cell secretion: vesicular exocytosis and oxidative stress. Chem Rev. 2008;108(7):2585–621.
69. Shen M, Colombo ML. Electrochemical nanoprobes for the chemical detection of neurotransmitters. Anal Methods. 2015;7(17): 7095–105.
70. Keighron JD, Ewing AG, Cans A-S. Analytical tools to monitor exocytosis: a focus on new fluorescent probes and methods. Analyst. 2012;137(8):1755–63.
71. Michael AC, Borland LM. Electrochemical Methods for neuroscience. Boca Raton: CRC Press/Taylor & Francis; 2007.
72. Gordito MP, Kotsis DH, Minteer SD, Spence DM. Flow-based amperometric detection of dopamine in an immobilized cell reactor. J Neurosci Methods. 2003;124(2):129–34.
73. Garris PA, Kilpatrick M, Bunin MA, Michael D, Walker QD, Wightman RM. Dissociation of dopamine release in the nucleus accumbens from intracranial self-stimulation. Nature. 1999;398(6722):67–9.
74. Zhang B, Heien MLAV, Santillo MF, Mellander L, Ewing AG. Temporal resolution in electrochemical imaging on single PC12 cells using amperometry and voltammetry at microelectrode arrays. Anal Chem. 2011;83(2):571–7.
75. Hashemi P, Dankoski EC, Lama R, Wood KM, Takmakov P, Wightman RM. Brain dopamine and serotonin differ in regulation and its consequences. Proc Natl Acad Sci. 2012;109(29):11510–5.
76. Amatore C, Arbault S, Bonifas I, Bouret Y, Erard M, Ewing AG, et al. Correlation between vesicle quantal size and fusion pore release in chromaffin cell exocytosis. Biophys J. 2005;88(6): 4411–20.
77. Wang K, Xiao T, Yue Q, Wu F, Yu P, Mao L. Selective amperometric recording of endogenous ascorbate secretion from a single rat adrenal chromaffin cell with pretreated carbon fiber microelectrodes. Anal Chem. 2017;89(17):9502–7.
78. Yin B, Barrionuevo G, Weber SG. Optimized real-time monitoring of glutathione redox status in single pyramidal neurons in organotypic hippocampal slices during oxygen-glucose deprivation and reperfusion. ACS Chem Neurosci. 2015;6(11):1838–48.
79. Andrews AM. Why monitor molecules in neuroscience? ACS Chem Neurosci. 2017;8(2):211–2.
80. Hu M, Fritsch I. Redox cycling behavior of individual and binary mixtures of catecholamines at gold microband electrode arrays. Anal Chem. 2015;87(4):2029–3.
81. Li X, Majdi S, Dunevall J, Fathali H, Ewing AG. Quantitative measurement of transmitters in individual vesicles in the

cytoplasm of single cells with nanotip electrodes. Angew Chem Int Ed. 2015;54(41):11978–82.
82. Takahashi Y, Shevchuk AI, Novak P, Zhang Y, Ebejer N, Macpherson JV, et al. Multifunctional nanoprobes for nanoscale chemical imaging and localized chemical delivery at surfaces and interfaces. Angew Chem Int Ed. 2011;50(41):9638–42.
83. Rees HR, Anderson SE, Privman E, Bau HH, Venton BJ. Carbon nanopipette electrodes for dopamine detection in drosophila. Anal Chem. 2015;87(7):3849–55.
84. Ren L, Pour MD, Majdi S, Li X, Malmberg P, Ewing AG. Zinc regulates chemical-transmitter storage in nanometer vesicles and exocytosis dynamics as measured by amperometry. Angew Chem Int Ed. 2017;56(18):4970–5.
85. Ye D, Gu C, Ewing A. Using single-cell amperometry and intracellular vesicle impact electrochemical cytometry to shed light on the biphasic effects of lidocaine on exocytosis. ACS Chem Neurosci. 2018;9(12):2941–7.
86. Li X, Dunevall J, Ewing AG. Electrochemical quantification of transmitter concentration in single nanoscale vesicles isolated from PC12 cells. Faraday Discuss. 2018;210:353–64.
87. Taleat Z, Larsson A, Ewing AG. Anticancer drug tamoxifen affects catecholamine transmitter release and storage from single cells. ACS Chem Neurosci. 2019;10(4):2060–9.
88. Welle Theresa M, Alanis K, Colombo ML, Sweedler JV, Shen M. A high spatiotemporal study of somatic exocytosis with scanning electrochemical microscopy and nanoITIES electrodes. Chem Sci. 2018;9(22):4937–41.
89. Kozminski KD, Gutman DA, Davila V, Sulzer D, Ewing AG. Voltammetric and pharmacological characterization of dopamine release from single exocytotic events at rat pheochromocytoma (PC12) cells. Anal Chem. 1998;70(15):3123–30.
90. Xin Q, Wightman RM. Enzyme modified amperometric sensors for choline and acetylcholine with tetrathiafulvalene tetracyanoquinodimethane as the electron-transfer mediator. Anal Chim Acta. 1997;341(1):43–51.
91. Mitchell KM. Acetycholine and choline amperometric enzyme sensors characterized in vitro and in vivo. Anal Chem. 2004;76(4):1098–106.
92. Bruno JP, Gash C, Martin B, Zmarowski A, Pomerleau F, Burmeister J, et al. Second-by-second measurement of acetylcholine release in prefrontal cortex. Eur J Neurosci. 2006;24(10):2749–57.
93. Giuliano C, Parikh V, Ward JR, Chiamulera C, Sarter M. Increases in cholinergic neurotransmission measured by using choline-sensitive microelectrodes: Enhanced detection by hydrolysis of acetylcholine on recording sites? Neurochem Int. 2008;52(7):1343–50.
94. Wilson GS, Johnson MA. In-vivo electrochemistry: what can we learn about living systems? Chem Rev. 2008;108(7):2462–81.
95. Asri R, O'Neill B, Patel JC, Siletti KA, Rice ME. Detection of evoked acetycholine release in mouse brain slices. Analyst. 2016;141(23):6416–21.
96. Colombo ML, Sweedler JV, Shen M. Nanopipet-based liquid–liquid interface probes for the electrochemical detection of acetylcholine, tryptamine, and serotonin via ionic transfer. Anal Chem. 2015;87(10):5095–100.
97. Iwai NT, Kramaric M, Crabbe D, Wei Y, Chen R, Shen M. GABA detection with nano-ITIES pipet electrode: a new mechanism, water/DCE–octanoic acid interface. Anal Chem. 2018;90(5):3067–72.
98. Stockmann TJ, Montgomery A-M, Ding Z. Determination of alkali metal ion transfers at liquid|liquid interfaces stabilized by a micropipette. J Electroanal Chem. 2012;684:6–12.
99. Zhan D, Li X, Zhan W, Fan F-RF, Bard AJ. Scanning electrochemical microscopy. 58. Application of a micropipet-supported ITIES tip to detect Ag+ and study its effect on fibroblast cells. Anal. Chem. 2007;79(14):5225–31.
100. Vanysek P, Ramirez LB. Interface between two immiscible liquid electrolytes: a review. J Chil Chem Soc. 2008;53:1455–63.
101. Shao Y, Mirkin MV. Voltammetry at micropipet electrodes. Anal Chem. 1998;70(15):3155–61.
102. Amemiya S, Kim J, Izadyar A, Kabagambe B, Shen M, Ishimatsu R. Electrochemical sensing and imaging based on ion transfer at liquid/liquid interfaces. Electrochim Acta. 2013;110:836–45.
103. Taylor G, Girault HHJ. Ion transfer reactions across a liquid—liquid interface supported on a micropipette tip. J Electroanal Chem Interfacial Electrochem. 1986;208(1):179–83.
104. Liu S, Li Q, Shao Y. Electrochemistry at micro- and nanoscopic liquid/liquid interfaces. Chem Soc Rev. 2011;40(5):2236–53.
105. Nestor U, Wen H, Girma G, Mei Z, Fei W, Yang Y, et al. Facilitated Li+ ion transfer across the water/1,2-dichloroethane interface by the solvation effect. Chem Commun. 2014;50(8):1015–7.
106. Amemiya S, Wang Y, Mirkin MV. Nanoelectrochemistry at the liquid/liquid interfaces. Electrochemistry. 2013;12:1–43.
107. Shen M, Chen R. Real time studies of acetylcholine release from single synapses and single cells with nanometer spatial resolution. In: Wilson GS, Michael AC, editors. Compendium of in vivo monitoring in real-time molecular neuroscience. Singapore: World Scientific; 2019. p. 161–78.
108. Haynes CL, Buhler LA, Wightman RM. Vesicular Ca2+ -induced secretion promoted by intracellular pH-gradient disruption. Biophys Chem. 2006;123(1):20–4.
109. Yang G, Gong Y-D, Gong K, Jiang W-L, Kwon E, Wang P, et al. Reduced synaptic vesicle density and active zone size in mice lacking amyloid precursor protein (APP) and APP-like protein 2. Neurosci Lett. 2005;384(1):66–71.
110. Thannickal VJ, Fanburg BL. Reactive oxygen species in cell signaling. Am. J. Physiol Lung Cell. Mol. Physiol. 2000;279(6):L1005–L28.
111. Sarti P, Avigliano L, Görlach A, Brüne B. Superoxide and nitric oxide–participation in cell communication. Cell Death Differ. 2002;9(10):1160–2.
112. Veal EA, Day AM, Morgan BA. Hydrogen peroxide sensing and signaling. Mol Cell. 2007;26(1):1–14.
113. Michaelson LP, Iler C, Ward CW. ROS and RNS signaling in skeletal muscle: critical signals and therapeutic targets. Annu Rev Nurs Res. 2013;31:367–87.
114. Thomas DD. Breathing new life into nitric oxide signaling: a brief overview of the interplay between oxygen and nitric oxide. Redox Biol. 2015;5:225–33.
115. Brown DI, Griendling K. Regulation of signal transduction by reactive oxygen species in the cardiovascular system. Circ Res. 2015;116(3):531–49.
116. Di Meo S, Reed TT, Venditti P, Victor VM. Role of ROS and RNS sources in physiological and pathological conditions. Oxidative Med Cell Longev. 2016;2016:1245049.
117. Finkel T, Holbrook NJ. Oxidants, oxidative stress and the biology of ageing. Nature. 2000;408(6809):239–47.
118. Waris G, Ahsan H. Reactive oxygen species: role in the development of cancer and various chronic conditions. J Carcinog. 2006;5:14.
119. Patten DA, Germain M, Kelly MA, Slack RS. Reactive oxygen species: stuck in the middle of neurodegeneration. J Alzheimers Dis. 2010;20(s2):S357–S67.
120. Heinecke JL, Ridnour LA, Cheng RYS, Switzer CH, Lizardo MM, Khanna C, et al. Tumor microenvironment-based feed-forward regulation of NOS2 in breast cancer progression. Proc Natl Acad Sci. 2014;111(17):6323–8.
121. Li Y, Sella C, Lemaître F, Guille-Collignon M, Thouin L, Amatore C. Electrochemical detection of nitric oxide and

peroxynitrite anion in microchannels at highly sensitive platinum-black coated electrodes. Application to ROS and RNS mixtures prior to biological investigations. Electrochim Acta. 2014;144:111–8.
122. Wang Y, Noël J-M, Velmurugan J, Nogala W, Mirkin MV, Lu C, et al. Nanoelectrodes for determination of reactive oxygen and nitrogen species inside murine macrophages. Proc Natl Acad Sci. 2012;109(29):11534–9.
123. Amatore C, Arbault S, Bouton C, Drapier J-C, Ghandour H, Koh ACW. Real-time amperometric analysis of reactive oxygen and nitrogen species released by single immunostimulated macrophages. ChemBioChem. 2008;9(9):1472–80.
124. Amatore C, Arbault S, Koh ACW. Simultaneous detection of reactive oxygen and nitrogen species released by a single macrophage by triple potential-step chronoamperometry. Anal Chem. 2010;82(4):1411–9.
125. Li Y, Hu K, Yu Y, Rotenberg SA, Amatore C, Mirkin MV. Direct electrochemical measurements of reactive oxygen and nitrogen species in nontransformed and metastatic human breast cells. J Am Chem Soc. 2017;139(37):13055–62.
126. Ikariyama Y, Yamauchi S, Yukiashi T, Ushioda H. Micro-enzyme electrode prepared on platinized platinum. Anal Lett. 1987;20(9):1407–16.
127. Ikariyama Y, Yamauchi S, Yukiashi T, Ushioda H. Surface control of platinized platinum as a transducer matrix for micro-enzyme electrodes. J Electroanal Chem. 1988;251(2):267–74.
128. Arbault S, Pantano P, Jankowski JA, Vuillaume M, Amatore C. Monitoring an oxidative stress mechanism at a single human fibroblast. Anal Chem. 1995;67(19):3382–90.
129. Li Y, Sella C, Lemaître F, Guille Collignon M, Thouin L, Amatore C. Highly sensitive platinum-black coated platinum electrodes for electrochemical detection of hydrogen peroxide and nitrite in microchannel. Electroanal. 2013;25(4):895–902.
130. Zhang X-W, Qiu Q-F, Jiang H, Zhang F-L, Liu Y-L, Amatore C, et al. Real-time intracellular measurements of ROS and RNS in living cells with single core–shell nanowire electrodes. Angew Chem Int Ed. 2017;56(42):12997–3000.
131. Slauch JM. How does the oxidative burst of macrophages kill bacteria? Still an open question. Mol Microbiol. 2011;80(3):580–3.
132. Dunevall J, Fathali H, Najafinobar N, Lovric J, Wigström J, Cans A-S, et al. Characterizing the catecholamine content of single mammalian vesicles by collision–adsorption events at an electrode. J Am Chem Soc. 2015;137(13):4344–6.
133. Lovrić J, Najafinobar N, Dunevall J, Majdi S, Svir I, Oleinick A, et al. On the mechanism of electrochemical vesicle cytometry: chromaffin cell vesicles and liposomes. Faraday Discuss. 2016;193:65–79.
134. Cheng W, Compton RG. Investigation of Single-Drug-Encapsulating Liposomes using the nano-impact method. Angew Chem Int Ed. 2014;53(50):13928–30.
135. Wang Y, Feng H, Zhang H, Chen Y, Huang W, Zhang J, et al. Nanoelectrochemical biosensors for monitoring ROS in cancer cells. Analyst. 2020. https://doi.org/10.1039/C9AN02390A.
136. Marquitan M, Clausmeyer J, Actis P, Córdoba AL, Korchev Y, Mark MD, et al. Intracellular hydrogen peroxide detection with functionalised nanoelectrodes. ChemElectroChem. 2016;3(12):2125–9.
137. Clausmeyer J, Actis P, Córdoba AL, Korchev Y, Schuhmann W. Nanosensors for the detection of hydrogen peroxide. Electrochem Commun. 2014;40:28–30.
138. Korchev YE, Gorelik J, Lab MJ, Sviderskaya EV, Johnston CL, Coombes CR, et al. Cell volume measurement using scanning ion conductance microscopy. Biophys J. 2000;78(1):451–7.
139. Amemiya S, Guo J, Xiong H, Gross DA. Biological applications of scanning electrochemical microscopy: chemical imaging of single living cells and beyond. Anal Bioanal Chem. 2006;386(3):458–71.
140. Kim J, Izadya A, Nioradze N, Amemiya S. Nanoscale mechanism of molecular transport through the nuclear pore complex as studied by scanning electrochemical microscopy. J Am Chem Soc. 2013;135(6):2321–9.
141. Maddar FM, Pery D, Brooks R, Page A, Unwin PR. Ananoscale surface charge visualization of human hair. Anal Chem. 2019;91(7):4632–9.
142. Takahashi Y, Hirano Y, Yasukawa T, Shiku H, Yamada H, Matsue T. Topographic, electrochemical, and optical images captured using standing approach mode scanning electrochemical/optical microscopy. Langmuir. 2006;22(2):10299–306.
143. Actis P, Tokar S, Clausmeyer J, Babakinejad B, Mikhaeleva S, Cornut R, et al. Electrochemical nanoprobes for single-cell analysis. ACS Nano. 2014;8(1):875–84.